ELECTROMAGNETIC CALCULATIONS FOR AN IMPROVED DESIGN OF THE MILAN K800 CYCLOTRON RF CAVITIES

L. Serafini, S. Gustafsson* and C. Pagani
University of Milan and INFN - Milan - Italy

Summary

This paper presents the results of the extensive calculations carried out for the optimization of the Milan K800 cyclotron RF cavities, using a special version of the computer code SUPERFISH[1]. A simulation, via a cylindrical symmetric model, of the cavity dee-liner region, has been developed. The procedure followed and its theoretical justification are sketched. Some new tools, useful for the design of the coaxial type cavities, are also presented.

Introduction

The three Milan RF cavities are essentially $\lambda/2$ non uniform coaxial lines, symmetrical with respect to the cyclotron median plane; they are fitted into the valleys of the pole tip, through axial holes in the magnet yoke[2]. The dee-liner region of the cavity, just around the symmetry plane, breaks up the cylindrical symmetry of the coaxial line in a very complicate geometry, since the dee profiles must follow the spiral edges of the sectors. The fundamental oscillation mode is still a typical coaxial TEM mode, to which the local evanescent TM waves (excited by the line discontinuities) are superimposed. The nominal frequency range is 15-48 MHz, achieved by means of two symmetrical sliding shorts varying the effective electrical length of the cavity. A cylindrical alumina insulator is also inserted in the coaxial line, in order to separate the vacuum part of the cavity from the air one, and to assure mechanical stability to the dee-stem, as can be seen in Fig.1. More details on the RF system can be found elsewhere[3].

Measurements performed on a prototype of the RF cavity have pointed out that the maximum resonating frequency was 47 MHz versus the anticipated 48 MHz. As a consequence, a detailed study of the electromagnetic fields behaviour inside the cavity became necessary, in order to achieve, via an optimization of the cavity geometry, an higher maximum frequency and, if possible, a better behaviour for some other critical quantities. These are: the electric field on the surfaces, the power consumption inside the cavity and the temperature raise of the ceramic insulator.

Simulation of the dee-liner region

Since the dee-liner region cannot be treated by a cylindrical symmetric calculation, it must be substituted by a cylindrical structure, which will be named simulating model, connected to the cavity coaxial part. In such a way the whole structure can be studied by means of a bidimensional finite element procedure, as the one carried out by the code SUPERFISH, which performs a discretization of the Helmoltz equation

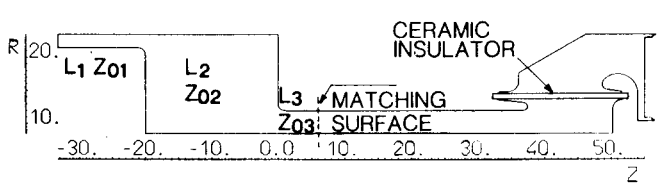

Fig.1 Schematic vertical cross section of the model cavity (see text for details).

$\nabla\times(\nabla\times H)=k^2\cdot H$ over an irregular triangular mesh (we used a minimum mesh size of 2 mm in the region close to the ceramic insulator, with a total number of about 20000 points inside the cavity).

In Fig.1 it is shown the schematic vertical cross section of the cavity coaxial part (positive z) and of the simulating model for the dee (negative z). The real cavity has been reduced to a $\lambda/4$ line, in the following indicated as "model cavity", which is terminated with an open end representing the symmetry plane (at z=-33.26).

An a priori knowledge of the frequency behaviour of the real cavity is however required in order to test the simulating model throughout the frequency range of the cavity. In our case a set of measurements on a cavity prototype were available, as can be seen in Fig.2, where the dots mark the short circuit position as a function of the resonance frequency. The simulating model has been designed in order to reproduce this curve: the dashed line of Fig.2 represents the calculated frequency behaviour of the model cavity.

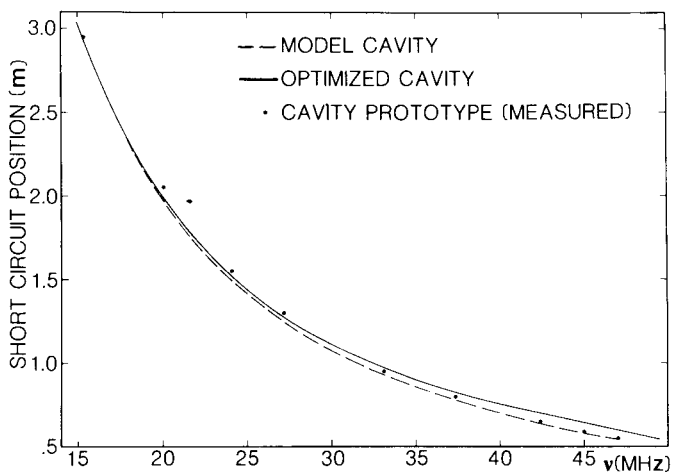

Fig.2 Short circuit position as a function of the resonance frequency for the measured data of the cavity prototype (dots), for the calculated model cavity (dashed line) and for the calculated optimized cavity (solid line).

The simulating model plays actually the role of generating, at each frequency between 15 and 48 MHz, the right boundary conditions on the matching surface, whose section is shown in Fig.1. The matching surface position has been fixed at a distance from the connection between the dee-liner region and the coaxial line, greater than the radii difference, so that the fields on this surface can be thought to be those typical of an uniform coaxial line. This choice turns out to be very powerful, since the value of the current at z=6. cm is sufficient, once given the normalization criteria (in our case 100 kV fixed on the open end), to completely specify the fields on the whole matching surface.

If the simulating model is able to reproduce the resonance condition for the model cavity, at the same frequency as the real cavity with the same short circuit position (and on the same $\lambda/4$ principal mode), the uniqueness theorem for e.m. fields[4] assures that the fields

* INFN - Catania - Italy

in the coaxial part of the cavity (up to the matching surface) are the same for the model cavity as for the cavity prototype. It is in fact always possible, simply applying a normalization factor to the fields of the model cavity, to obtain a current at the matching surface position equal to that one of the cavity prototype at this point. Since the tangential electric field is zero on the metal boundary (which are considered as perfectly conductive), the tangential components of the fields, on the close surface enclosing the coaxial part of the cavity, turn out to be coincident for the two cavities, as required by the theorem.

The fields are also uniquely defined for the simulating model, once given the current at the matching surface position (at a fixed frequency). This fact is of great importance, since it allows to apply all the needed corrections on the coaxial part of the cavity, which leave unchanged the resonance frequency, without destroying the validity of the simulation. Clearly the matching surface fields must not be perturbed: this is assured if no discontinuities in the coaxial region are placed at a distance from the matching position lower than the radii difference.

If the frequency does not vary, even with different geometries of the coaxial region, the fields inside the simulating model are unchanged (apart the normalization factor); the model therefore represents still the dee-liner region contribution, at that specified frequency. From this point of view, the simulation turns out to be simply a reproduction, at each frequency, of the correct fields on the matching surface, i.e. of the correct impedance at z=6. cm.

The importance to fit the frequency behaviour of the real cavity, throughout the whole frequency range, by means of one fixed simulating model, is therefore due to the possibility to vary the geometry of the coaxial region, i.e. to change the relation between the short circuit position and the resonance frequency, leaving unchanged the validity of the simulating model. This is true if the simulating model is not dependent on the frequency: in this case it gives automatically, at each frequency, the correct impedance on the matching surface. Moreover, due to the good fit of the real cavity behaviour in the high frequency region (see Fig.2), a slight extrapolation just off the fitting range, toward higher frequencies, should not affect the accuracy of the simulation.

This is no more true for higher oscillating modes of the cavity: nothing assures that the simulation is still valid also for frequency far from the fitting range. We could, in principle, analyze only the higher modes of the $(2n+1/4)\lambda$ type with frequency not much higher than 50 MHz. Since the lower frequency for these modes has been found at 57.8 MHz, with a short circuit position at z=303 cm, we renounced to develop a complete study on this problem, due to the uncertainty affecting the frequency value (hence the distribution of the fields in the whole cavity).

The procedure followed for the design of the simulating model is extensively reported elsewhere[5]. Here we recall the general scheme: a model formed by three lines with different length (L_1,L_2,L_3) and characteristic impedance (Z_{o1},Z_{o2},Z_{o3}) has been chosen. The parameters being left to vary were L_1,L_2,Z_{o1} (see Fig.1): they were optimized in order to reproduce, at the matching position, the right impedance as a function of the resonance frequency $Z_m(\omega)=V_m(\omega)/I_m(\omega)$ (this function has been evaluated at some frequencies connecting an uniform coaxial line at the coaxial part of the cavity and calibrating its length in order to produce the resonance at the frequency value corresponding to the chosen short circuit position, as prescribed by the experimental data).

Since the matching surface has been taken inside an uniform coaxial line, the impedance, at the resonance, can be written as $Z_m(\omega)=-j\cdot Z_{o3}\cdot\cot\alpha_m(\omega)$, with $Z_{o3}=20.67$ ohm. In Fig.3 the impedance amplitude $Z_m(\omega)$ and the phase advance $\alpha_m(\omega)$ at the matching surface are plotted (the phase advance $\alpha(\omega)$ varies along the cavity from 0° at the open end to 90° at the short circuit). The not linear trend of the function $\alpha_m(\omega)$ excludes the possibility to use an uniform coaxial line as a simulating model: the α_m produced by such a model would be in fact given by $\alpha_m = k\cdot L$, where L is the coaxial length and $k=\omega/c$. An iterative search has been performed on the three free parameters in order to reproduce $\alpha_m(\omega)$ at the matching surface.

However the starting choice for the search has been given by a first order approximation for $\alpha_m(\omega)$, which is represented by the sum of the contributions coming from the three uniform lines $\Delta\alpha_i = k\cdot L_i$ and the contributions coming from the two discontinuities in the characteristic impedance at z=-20 cm and z=0 cm. At each discontinuity the formula[5]:

$$\alpha_b = \operatorname{atan}\left[\frac{Z_{oi}}{Z_{oi-1}}\cdot\tan\alpha_f\right] \qquad i=2,3$$

must be applied (refer to Fig.4 for the related quantities). Since α_m is given by this approximation as a function of the three free parameters, it is possible to choose their values in order to fit the function $\alpha_m(\omega)$ of Fig.3. Generally the starting values thus obtained for L_1,L_2,Z_{o1} are varied by less than 10% by the following iterative search (performed with successive designs tested by SUPERFISH runs). It should be noted that the presented approximation on the impedance behaviour along the line is fully consistent with the constant impedance element approach, hence it does not take into account the effect of the local evanescent TM waves excited by each discontinuities, which are instead fully described

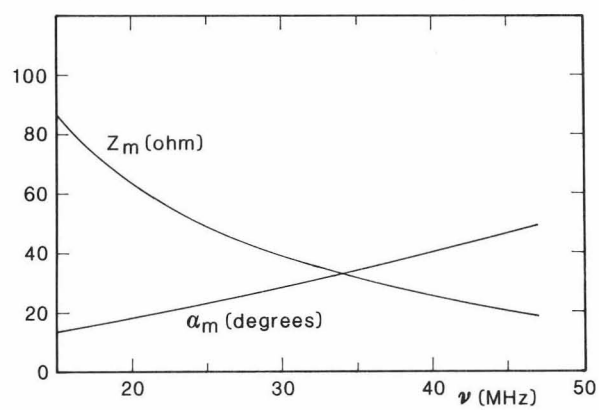

Fig.3 Impedance amplitude and phase advance at the matching surface as functions of the resonance frequency.

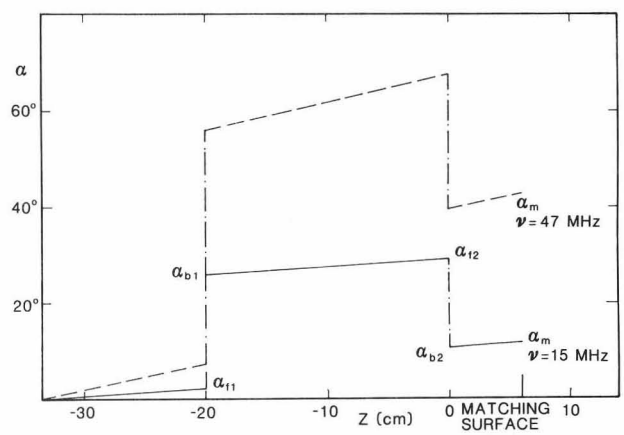

Fig.4 Phase advance of the impedance inside the simulating model, for the two indicated frequencies, as given by a constant impedance element approach (see text for details).

by the SUPERFISH calculations.

As a conclusion, the quantities related to the fields distribution in the coaxial part of the cavity (like power dissipation in the ceramic, electric field on the corona rings, frequency variation due to change of geometry) are the same for the model cavity and for the cavity prototype (within the accuracy of the fields description given by the finite element procedure). On the contrary, the quantities which take into account the contribution coming from the fields in the whole cavity (like Q, power dissipation, shunt impedance) are described with a lower accuracy, since they depend on the actual shape of the simulating model, which is not uniquely defined (we looked for a simulating model able to reproduce, at 100 kV voltage on the open end, the expected short circuit current from constant impedance element computations). However, all the variations of each of these quantities, due to change of the coaxial region geometry, depend only on the fields inside the coaxial region, hence are described with the accuracy of the finite-element code. For this reason, even if the absolute value of the power dissipation is known with a 10% error, it is possible to check very precisely the relative change of this quantity, when some corrections are applied to the coaxial region.

Optimization of the cavity geometry

It is well known that a correction of the cavity geometry which reduce the cavity volume in its inductive region (i.e. in the neighborhood of the short circuit) increases the resonance frequency, according to the formula:

$$\frac{\Delta\omega}{\omega} = \int_{\Delta V} \frac{(\mu H^2 - \varepsilon E^2)}{4U} dV \qquad (1)$$

which gives, in a perturbative approximation, the frequency shift due to the removal of a small volume ΔV from the cavity (U is the total energy stored). Consequently, a tapering of the inner and outer coaxial in the region close to the ceramic insulator has been designed to enhance the maximum frequency. In designing the new coaxials, the behaviour of three critical quantities must be however taken into account:

- the electric field on the surface of the upper corona ring (in air) must be below the sparking limit of 30 kV/cm
- a significant increase of the power dissipated in the cavity must be avoided
- the power dissipation in the ceramic insulator should not produce a significant temperature raise (i.e. larger than 50 °K)

The final design is presented in Fig.5, where the profiles of the cavity prototype and of the optimized cavity are plotted; the dashed regions mark the volume reductions. The shift of the upper and lower housings for the ceramic insulator are due to an improvement of the upper corona ring cooling[6]. The large reduction of the lower corona ring is needed in order to reduce the electric field on its surface and the temperature raise

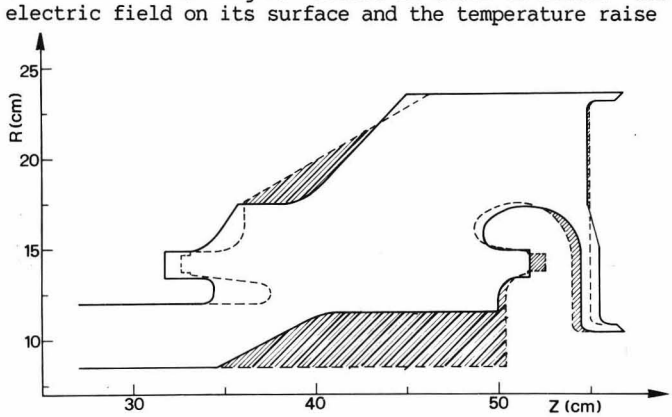

Fig.5 Cavity boundary of the model cavity (dashed line) and of the optimized cavity (solid line) : the short circuit shown on the right is at the minimum distance from the corona ring in both cases.

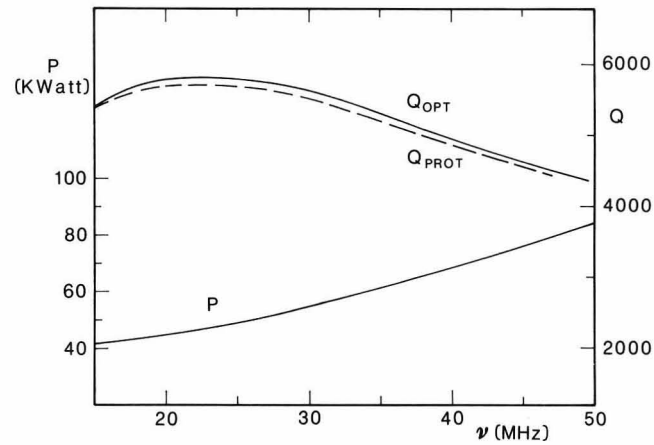

Fig.6 Power dissipation and quality factor as functions of the frequency for the model cavity (dashed line) and for the optimized cavity (solid line).

of the insulator, as will be shown later.

The frequency behaviour of the optimized cavity, as calculated with SUPERFISH, is plotted in Fig.2 (solid line): a larger frequency range (15-49.5 MHz) has been achieved with the same excursion of the short circuit. The perturbation on the resonance frequency produced by the tapers, which is of the order of +5% at 47 MHz, is strongly reduced, at the low frequencies, where the energy stored in the cavity is almost doubled with respect to the maximum frequency. Moreover, the volume ΔV of eq. (1), corresponding to the coaxials tapers, shifts progressively, with decreasing the frequency, toward the middle of the cavity, where the magnetic and electric energy density are nearly equal.

The energetic behaviour of the cavity is shown in Fig.6, where the calculated power dissipation of the whole $\lambda/2$ optimized cavity is plotted versus the frequency for the case of 100 kV voltage on the open end (the same quantity for the model cavity follows a curve which is not distinguishable). The power is computed actually in a perturbative approximation: the H field calculated by SUPERFISH corresponds to perfect conducting boundaries, but the induced current on the cavity walls are taken into account to integrate the dissipation inside the skin depth over the whole cavity surface (a 15% increase of the normal copper resistivity has been taken to include a safety margin on the power). The quality factor Q is also plotted: the slight increase for the Q of the optimized cavity is due to the decrease of the overall current path length on the cavity surface.

The electric field on the surface of the coaxials in the region close to the ceramic insulator are shown in Fig.7. The arrows represent just the electric field vectors on the surface points; each segment marked by the scales on the arrows represents a field value of 10 kV/cm. The electric field amplitude is computed by the relation $E = (1/rk\varepsilon_r)\cdot\partial(r\cdot H)/\partial l$, l being the path coordinate along the cavity boundary (H in suitable units): the electric field values take therefore into

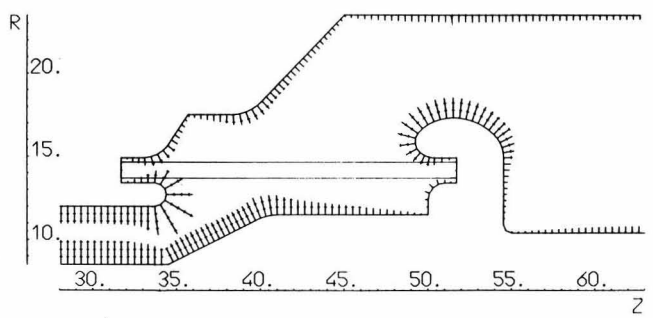

Fig.7 Electric field vectors on the surface of the cavity in the corona rings region.

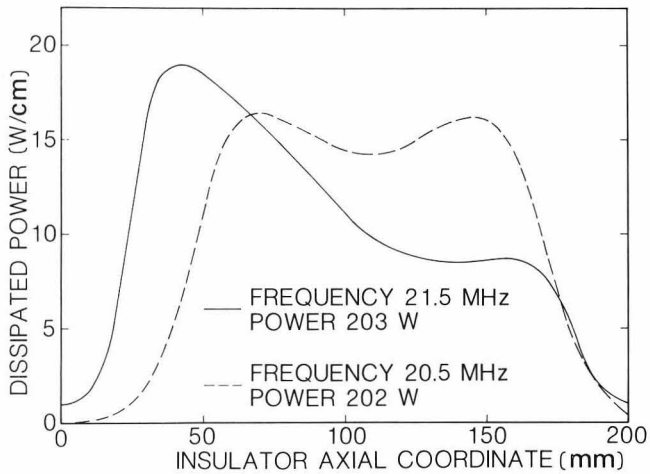

Fig.8 Linear density of the power dissipated inside the ceramic insulator, as a function of its axial coordinate, for the model cavity (dashed line) and for the optimized cavity (solid line) at the indicated frequencies

account the variation along the cavity of the voltage difference between the two coaxials. The maximum electric field in the air region is ≃27 kV/cm on the upper corona ring (at the lowest frequency, 15 MHz). This quite comfortable value has been obtained with a careful optimization of the corona ring contour, which is composed by six tangentially connected arcs of different curvature.

In Fig.8 the dissipated power in a cylindrical strip (Δr=1 cm, Δz=1 cm) of the ceramic insulator is shown as a function of its axial coordinate, for the cavity prototype (dashed line) and for the optimized cavity (solid line). The origin of the abscissa scale corresponds to the bottom of the insulator housing formed by the lower corona ring (z=31.7 cm for the optimized cav. and z=32.15 cm for the prototype cav.). The chosen frequencies are those ones of maximum power dissipation inside the ceramic insulator, for both cases. The total dissipated power is computed according to the relation:

$$P_{cer} = \frac{\omega \varepsilon_o \varepsilon_r}{2Q_{cer}} \cdot \int_V E^2 dV \qquad (2)$$

where V is the insulator volume and Q_{cer} is the ratio of the real part versus the imaginary one of the dielectric constant (in our case ε_r=10 and Q_{cer}=10000, from conservative Wessgo specs). The strong shift of the peak in the power density for the optimized cavity toward the low zeta, shown in Fig.8, is mainly due to the reduction of the lower corona ring and to the presence of the inner tapering: the total power is practically unchanged. In fact, since the upper corona ring region has been estimated to be 20°K hotter[6] than the lower corona ring, the not symmetrical behaviour of the power density has the nice effect to decrease the maximum temperature raise in the ceramic insulator, as can be seen in Fig.9, where the temperature of each point in the ceramic insulator is plotted. The temperature curves have been computed integrating the heat diffusion equation in the axial direction throughout the insulator.

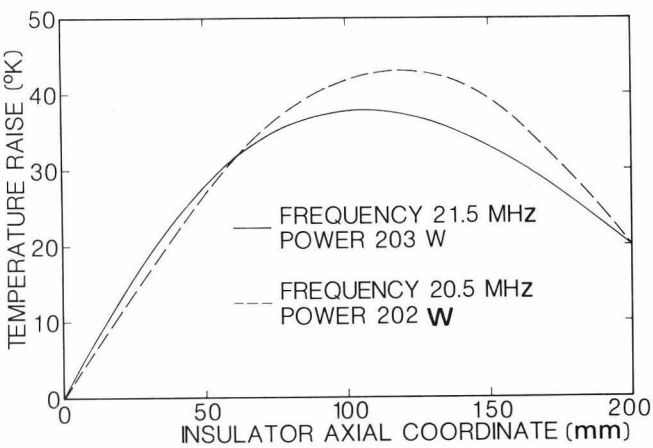

Fig.9 Temperature raise distribution inside the ceramic insulator, as a function of the insulator axial coordinate, for the model cavity (dashed line) and for the optimized cavity (solid line), at the indicated frequencies.

Some new tools for the design of a coaxial type cavity

The code SUPERFISH, a powerful computer program for the study of RF cavities, has been equipped in our laboratory with a number of related routines which have been revealed very useful in the design of the coaxial type cavities.

The calculation of the power dissipated in pieces of dielectric material inserted in the cavity and their temperature raise has been already illustrated. A similar calculation for ferrites is also straightforward. The presented plots for the electric field on the cavity surfaces are also useful to look quickly at the field distribution.

The conventional method followed to represent the fields pattern of a TM mode (as in our case where $\mathbf{E}\equiv(E_r,0,E_z)$ and $\mathbf{H}\equiv(0,H_\phi,0)$) consists in tracing the lines defined by the equation $r\cdot H_\phi = \text{const} = I_1/2\pi$ (in the following simply called rH lines). If the difference in the linked current I_1 between any two consecutive lines is constant, then this is a system of electric field lines. The electric field is tangential to each line and the density of the system of lines is proportional to the field amplitude times the radius (as usual in a cylindrical geometry), according to the relation $r|\mathbf{E}| = |\nabla(rH_\phi)|/(k\varepsilon_r)$. An example is given in Fig.10, where these lines are plotted for the optimized cavity

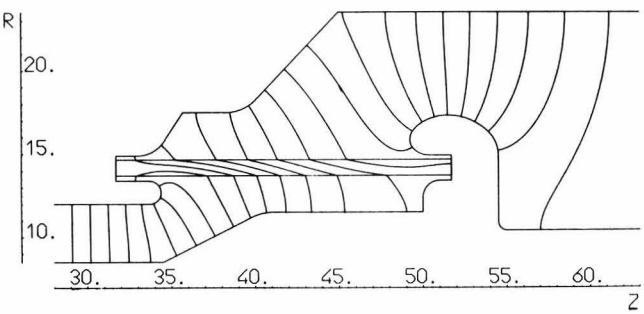

Fig.10 Electric field lines plotted at a constant increase of the linked current, at a resonance frequency of 32.2 MHz

at ν=32.2 MHz. Each line marks a specified level of the linked current, and they are spaced at a constant increase of the linked current.

An alternative field pattern is presented in Fig.11. Here two orthogonal systems of lines are plotted. The first one consists of rH lines which are spaced at a constant increase of the voltage difference between the two coaxials, calculated along an electric field line. The second one is defined by the lines connecting the points of each rH line which have the same fraction of the voltage difference with respect to the total voltage difference seen along the line. Let

$$V_p = \int_{L,P_1}^{P} \mathbf{E}\cdot d\mathbf{l} \quad \text{and} \quad V = \int_{L,P_1}^{P_2} \mathbf{E}\cdot d\mathbf{l} = \frac{1}{k\varepsilon_r}\int_S H_\phi da \quad (\mathbf{E} = \nabla \mathbf{x} \mathbf{H}/k\varepsilon_r)$$

where L is a rH line, and S is the surface enclosed by the line L and the boundary of the cavity on the side of the short circuit (V is actually computed with the surface integral on the magnetic field, since H is the

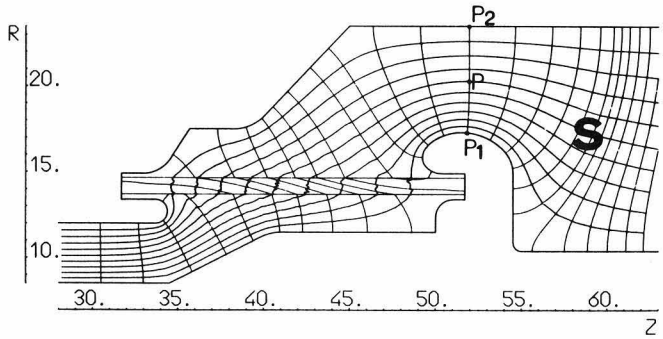

Fig.11 Electric field lines plotted at a constant increase of the voltage difference seen along a line, for the case of ν=32.2 MHz. The orthogonal system of lines (called equipartitional lines) is also shown.

primary quantity computed by the finite element procedure, while **E** must be computed by a numerical derivation).

The equation V_p/V = const. defines then the second system of lines, which we called equipartitional lines. The function V_p/V corresponds, in the dynamic case, to the potential function in an electrostatic situation. It can be shown that the lines V_p/V = const are orthogonal to the electric field lines, their mutual distance is proportional to the amplitude of **E**, and each curvilinear square of the grid formed by the two systems of lines has a constant linked magnetic flux. All these properties should offer the possibility of a very powerful definition for the generalized characteristic impedance along the cavity as a function of the wave phase advance. An useful property of the equipartitional lines (which actually represent the section of the corresponding revolution surfaces) is that any cavity made of perfect conducting walls coincident with any two of the corresponding revolution surfaces, still resonates at the same frequency as the actual cavity. This property can be simply demonstrated applying again the uniqueness theorem.

Another interesting picture, which allows to see at a glance the frequency shift produced by any perturbation on the boundary of a coaxial cavity, is presented in Fig.13. Here the numbers on the lines indicate the frequency shift (in kHz/cm^2) due to a 1 cm^2 reduction of the cavity area in the r-z section. The line equation is (from eq. (1)) $\pi\nu r(\mu H^2-\varepsilon E^2)/(2U)$ = const., the constant being shown on each line. This system of lines (we called it the "fan", due to its similarity to a fan when it is plotted in an uniform coaxial, as shown in Fig.12) is very useful to evaluate quickly the effect on the resonance frequency of any tapering applied to the cavity, simply adding the contribution of each elementary (1 cm^2 area) square in which the tapering can be subdivided (a similar evaluation has been tested, for the case of the inner and outer tapering applied to the model cavity, reaching an accuracy of about 10% against the frequency change actually computed with SUPERFISH). The regions of the cavity which are most sensitive to frequency shift are moreover efficiently enlightened.

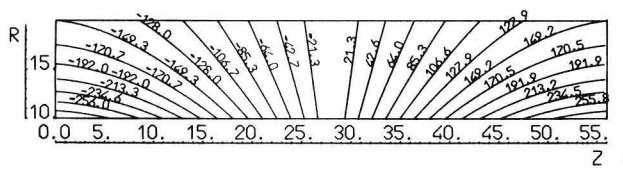

Fig.12 The "fan" lines plotted in a uniform λ/4 coaxial cavity, with the open end at z=0. cm and the shorted one at z=56. cm. Positive and negative values on the lines mark the inductive and capacitive regions (respectively) of the cavity (see text for details).

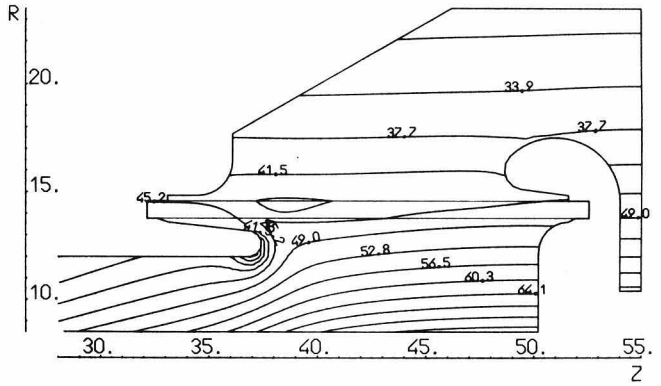

Fig.13 The "fan" lines plotted in the ceramic insulator region of the model cavity at ν = 47 MHz. The numbers shown on the lines give the shift of the resonance frequency, in a perturbative approximation (see text for details).

Conclusions

Once understood the role of the simulation, via a bidimensional model, of the dee-liner region, it becomes feasible the design of the whole coaxial part of the cavity only on the basis of the calculated fields. So that it would have been possible to build a very simple shorted coaxial line, connected to the dee-liner region as shown in Fig.14, in order to test a simulating model inside the achieved frequency range, after measuring at low power the frequency versus the short circuit position (the proposed geometry resonates between 15 and 80 MHz with a very short excursion of the short circuit).

The actual shape of the coaxial part of the cavity, once a simulating model is available, can be consequently designed according to the imposed requirements on the power dissipations, electric field behaviour, and frequency range needed, just by studying the computed fields, with no needs of a full cavity prototype.

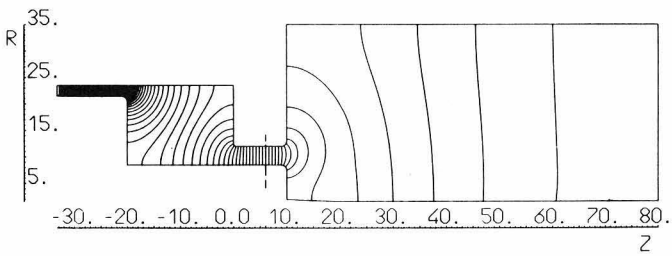

Fig.14 Vertical section of a simple coaxial line (the matching surface section is shown) resonating at 20 MHz, useful to perform low power measurements on the frequency for the test of a simulating model (see text for details).

References

1) K. Halbach and R.F. Holsinger, SUPERFISH - A computer program for the evaluation of RF cavities with cylindrical symmetry, Particle Accelerators, 1976, vol. 7, No. 4, pag. 213
2) E. Acerbi et al., Progress report on the Milan superconducting cyclotron, this conference
3) C. Pagani et al., Proc. 10th Int. Conf. on Cycl. and their Appl., East Lansing 1984, IEEE catalog N. 84CH 1966-3, pag. 305
4) R.E.Collin, Field theory of guided waves, McGraw-Hill (New York) 1960, p. 27
5) L. Serafini et al., A model approach for the non uniform coaxial cavities, to be published
6) C. Pagani, Full power tests of the first RF cavity for the Milan K800 cyclotron, this conference
7) L. Serafini et al., Special field patterns for coaxial type cavities, to be published